Radiation forces associated with heat propagation in nonisothermal systems

F. S. Gaeta and E. Ascolese
International Institute of Genetics and Biophysics of Consiglio Nazionale delle Ricerche, Via G. Marconi 10, Naples, Italy

B. Tomicki
Institute of Biology and Biophysics of Agricultural, University of Wroclaw, Uliza Norwida 25, Wroclaw, Poland
(Received 6 August 1990)

The aim of this work is to show that, in the condensed phases, the flux of thermal energy couples with a flux of momentum. This follows from considerations of rational mechanics and can be also deduced as a corollary of a theorem established by Boltzmann, following a straightforward reasoning already developed by Ehrenfest in a somewhat simpler case than the one considered by us. When heat flux crosses the boundary between two adjoining media, the momentum flux changes, and "thermal radiation forces" should appear. Accordingly, the momentum-balance equation of continuous-field hydrodynamics should include, when applied to nonisothermal media, the momentum flux due to heat flow. When this is done, analytical expressions for thermal radiation forces are obtained with reference to various simple physical systems. The theoretical predictions lend themselves to direct experimental verification. Very good qualitative and quantitative agreement between theory and experiment has been found in various experimental systems, as described here, lending strong support to the proposed approach. Interestingly, experimental results obtained with macroscopic objects and with molecular or ionic particles both lead to analogous conclusions concerning the properties of thermal radiation forces, a circumstance that broadens the possible field of application of these concepts. Finally, it is suggested that the concept of momentum flux coupled to transport of thermal energy in the condensed phases can be fruitfully employed in the investigation of complex phenomena such as acoustic streaming and the Bérnard-Rayleigh instabilities.

PACS number(s): 47.10.+g, 03.40.Kf, 62.30.+d, 65.90.+i

I. INTRODUCTION

Radiation pressures resulting from wave propagation are known in a variety of different physical situations. A radiation pressure occurs in electrodynamics, the Maxwell stress tensor being used to describe the force exerted on an object by electromagnetic waves. Mechanical radiation pressure also occurs in acoustics, where waves exert forces on obstacles: the force per unit area being proportional to the energy density of the impinging mechanical radiation. This form of radiation pressure has been extensively studied since the pioneering work of Rayleigh [1,2] and, although the literature is full of errors, satisfactory treatments of various aspects of the problem do exist [3–11]. The tensorial character of the so-called "radiation pressure" in the condensed phases was initially pointed out by Brillouin in 1925 [3]. The importance of considering the density of flux of momentum coupled to the energy flux has been demonstrated by Borgnis [7] and Johansen [9]. Suggestive generalizations of the concept are due to Lucas [5], who measured radiation forces produced by fluxes of thermal rather than acoustic energy.

On the other hand, very little attention has been paid to either the phenomenology or the theory of radiation stresses in nonisothermal media. Actually, modern developments of rational mechanics of continuous media, principally those due to Truesdell and Noll [12], formally couple momentum flux to the flux of thermal energy, without leading to insight into the underlying physical mechanisms. The lack of an adequately broad theoretical basis and the smallness of known effects of nonisothermal matter transport, reduced interest in the field or induced completely different approaches. Efforts to explain thermal diffusion in liquids, for instance, generally took the form of modifications of the kinetic theory of gases.

A simple theory of the thermomechanical effect was developed by one of us [13] by invoking analogous situations from acoustics—i.e., momentum carried by ultrasonic waves in elastic media. In the course of subsequent experimental studies, supporting evidence has been obtained confirming the theoretical expectations [14–18]. Other situations in which the heat flux couples with transport of matter or produces sizable hydraulic pressure have also been experimentally investigated [19–24]. Thus the idea that thermal energy propagating in condensed matter generates radiation pressure rests by now on a sufficiently broad experimental basis. On the other hand, membrane systems yielding the most convincing evidence are structurally complex and operate under nonlinear conditions, the observed effects being obtained by applying very large temperature gradients across thin porous membranes, thus generating intense heat fluxes within their liquid-filled pores [23,24]. A straightforward quantitative comparison of these experimental results with theory is therefore not yet feasible at present. With this work we propose a more satisfactory form of the theory of radiation forces due to heat propagation, which follows from a simple application of a theorem due to Boltzmann and, alternatively, can be also deduced from

an application of the momentum-balance equation to a system through which heat is flowing. We also discuss here accurate experimental results recently obtained in our laboratory employing a simple system that allows comparison with the theory; finally we present a critical discussion of some well-known experimental articles of other authors whose puzzling results may be simply interpreted in terms of the thermal-radiation-force theory.

When heat propagates in an anisotropic medium, the flux of thermal energy $\mathbf{J}_q$ is connected with the temperature gradient by the thermal conductivity tensor K, the phenomenological equation being $\mathbf{J}_q = -\mathrm{K}\cdot\mathrm{grad}T$ (Fourier). According to our working hypothesis then the propagation of momentum carried by thermal energy shall be described by a momentum flux tensor J_p constituted by the dyadic product of momentum density $\mathbf{g}$ and velocity of propagation of phononic excitations $\mathbf{u}$, namely $\mathrm{J}_p = \mathbf{gu}$. Momentum density is related to energy flux by the relation $\mathbf{g} = \mathbf{J}_q / u^2$, similar to energy and momentum of sound waves [13]; thus we have

$$\mathrm{J}_p = \mathbf{gu} = \frac{\mathbf{J}_q}{u}\frac{\mathbf{u}}{u} = \mathbf{J}_p\mathbf{n} \ , \tag{1}$$

where $\mathbf{n}$ is the unit vector along $\mathbf{u}$, and

$$\mathbf{J}_p = \frac{\mathbf{J}_q}{u} = -\frac{\mathrm{K}}{u}\cdot\mathrm{grad}T \tag{2}$$

is the momentum flux due to the flux of thermal energy.

Thus, whenever one considers the mechanics of a nonisothermal system, the momentum flux coupled to the heat flux must be allowed for. In particular, the momentum-balance equation of hydrodynamics must include the thermal-radiation stress tensor.

The use of Fourier phenomenological law in this context, where reference is made to thermal excitations propagating with finite velocity $\mathbf{u}$, may seem contradictory. A more general constitutive approach using, e.g., the Maxwell-Cattaneo equation [25,26] $\tau_r(d\mathbf{J}_q/dt) + \mathbf{J}_q = -\mathrm{K}\cdot\mathrm{grad}T$ looks to be more appropriate. Here τ_r is a relaxation time connected with the finite propagation velocity of thermal excitations. However, in this paper we are dealing only with steady-state situations, where the Maxwell-Cattaneo equation reduces to the classical Fourier expression. Radiation-pressure effects appearing in the transient behavior, connected through the relaxation time τ_r, shall be dealt with in a separate paper.

II. THERMAL RADIATION FORCES AND A BOLTZMANN THEOREM

We shall now try to establish Eq. (2) on a firmer physical basis, by deriving the expression for the momentum flux coupled to heat flow directly from a theorem of Boltzmann [27]. This theorem was subsequently applied by Ehrenfest to the adiabatic condition. We will consider boundary conditions slightly more general than those assumed by Ehrenfest, and also carry our analysis one step further.

Let us consider a system consisting of an isotropic medium made by a great number of particles interacting among them through forces limiting the total number of degrees of freedom. The system can vibrate at many characteristic frequencies, and, at any temperature above absolute zero such vibrations spontaneously occur, even in the absence of external excitation. If an amount ΔQ of thermal energy is added to the system, the Boltzmann theorem states that

$$\Delta Q = \frac{2}{\tau}\delta\int_0^{\tau} E_{\mathrm{kin}}\,d\tau = \frac{2}{\tau}\delta(\langle E_{\mathrm{kin}}\rangle_\tau \tau) \ , \tag{3}$$

where $\langle E_{\mathrm{kin}}\rangle_\tau$ is the average kinetic energy associated with vibrations of period τ. Ehrenfest considers the particular case of an adiabatic system, not exchanging heat with its surroundings. We instead focus our attention on a system at thermal steady state, where the condition $\Delta Q = 0$ follows from the equality of entering and issuing heat fluxes. Such is, for instance, the case of an isotropic condensed phase—say a cylinder of homogeneous liquid which is thermally insulated on a lateral surface, while a steady heat flux enters and, respectively, emerges from its upper and lower faces (see Fig. 1), due to a temperature difference along x. Once thermal effects connected with the initial transient are over, the net exchange of thermal energy of the system with the external world is equal to zero over any time interval, as in the adiabatic case, and from Eq. (3) for each value of τ one then has

$$\delta(\langle E_{\mathrm{kin}}\rangle_\tau) = 0, \quad \text{i.e.,} \ \langle E_{\mathrm{kin}}\rangle_\tau \tau = \text{const along } x. \tag{4}$$

The thermodynamic difference, of course, is that here there is a constant rate of entropy production in the system due to the steady-state flux of thermal energy, a circumstance, however, that does not affect the form of Eqs. (3) and (4). Elastic vibrations in the medium may be considered to satisfy locally the relation

$$\langle E_{\mathrm{kin}}\rangle_\tau = \langle E_{\mathrm{pot}}\rangle_\tau = \tfrac{1}{2}U \ , \tag{5}$$

$\langle E_{\mathrm{pot}}\rangle_\tau$ being the average potential and U the total mechanical energy connected to oscillations. (For a discussion of this point see Appendix A). From Eqs. (4) and (5) then it follows

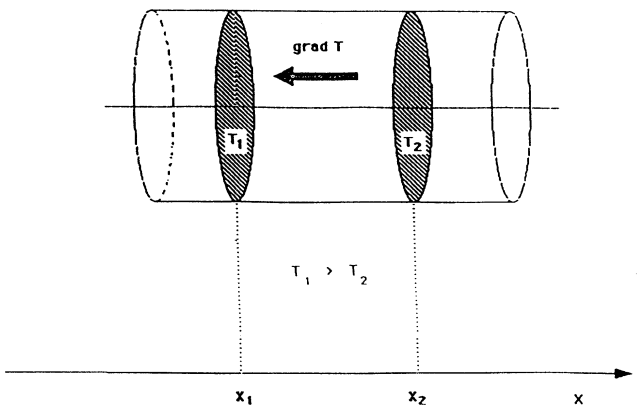

FIG. 1. Cylindric portion of an homogeneous liquid thermally insulated on its lateral surface. A temperature gradient is applied along its axis x producing a steady heat flux in the medium.

$$\frac{1}{\tau}\frac{d\tau}{dx}+\frac{1}{U}\frac{dU}{dx}=0\ . \tag{6}$$

This means that every change of local vibration frequency will be connected with a variation of mechanical energy U. More specifically, the percent variation of the period shall be equal and opposite to that of the mechanical energy.

It is well known that thermal energy in the condensed phases mostly consists of very-high-frequency elastic waves. Part of the spectrum of these phonon-type thermal excitations has been experimentally investigated in liquids via optical methods [28–33]. Proceeding from a region of the liquid to another that is hotter or cooler, the waves undergo frequency changes due to thermal expansion.

On the other hand, Eq. (6) allows us to write

$$dL\equiv F\,dx=-dU=U\frac{d\tau}{\tau}=S\left[\frac{U}{S\tau}\right]d\tau\ , \tag{7}$$

where S is the cylinder cross section. Thus mechanical work is produced by the system when thermal excitations drift down the temperature gradient. Since we are considering steady-state conditions, every production of work connected with the transient must have disappeared. So the work dL can be due only to energy dissipation connected with the heat propagation in the medium. We see that the temperature gradient affects the elastic properties of the medium which now change along x while, at the same time, it also affects the dynamics of the population of thermal phonon excitations, producing a net drift of the excitations along this same axis. The quantity $U/S\tau$ represents mechanical work per unit of surface produced in the medium per period, when heat—in the form of high-frequency elastic-waves—propagates along x. Obviously, $U/S\tau$ is proportional to heat flux, i.e., to the equidimensional quantity $J_q=-K(dT/dx)$, K being the tensor thermal conductivity, reduced here to a simple function of x. We may then write

$$dL=S\left[\frac{U}{S\tau}\right]d\tau=S\left[-K\frac{dT}{dx}\mathcal{R}\right]\frac{d\tau}{dx}dx\ , \tag{8}$$

$\mathcal{R}$ being an a-dimensional proportionality constant connecting $U/S\tau$ and J_q within dx. The physical meaning of $\mathcal{R}$ is that of a reflection coefficient due to the nonisothermal condition, defined by

$$\mathcal{R}\equiv\left[\frac{d(\rho u)}{\rho u+\rho u+d(\rho u)}\right]^2\ , \tag{9}$$

where ρu is acoustical impedance of the medium. Thus wave reflection is seen as due to the gradual change of density and sound velocity brought about by temperature change along x rather than by abrupt discontinuity as in the case of acoustic radiation pressure. We shall discuss this point further elsewhere [34].

Let us now proceed in considering what occurs when thermal excitations drift from x_1 to x_2 (Fig. 1). The work $L_{(x_1,x_2)}$ shall be given by

$$L_{(x_1,x_2)}=-S\mathcal{R}\int_{x_1}^{x_2}K\frac{dT}{dx}\frac{d\tau}{dx}dx$$
$$=-S\mathcal{R}K\frac{dT}{dx}\int_{x_1}^{x_2}\frac{d\tau}{dx}dx\ , \tag{10}$$

where $K(dT/dx)$, being invariant along x, can be taken out of the integral. It should be noted that now $\mathcal{R}\equiv(\rho_2u_2-\rho_1u_1/\rho_2u_2+\rho_1u_1)^2$, where $(\rho u)_{x_1}\equiv\rho_1u_1$ and $(\rho u)_{x_2}\equiv\rho_2u_2$.

On the other hand, τ is connected with phase velocity by $\tau=2\pi h_0/u$, where h_0 is intermolecular distance in the medium at 0 K. (See the Appendix for a discussion of this point). We thus have

$$\int_{x_1}^{x_2}\frac{d\tau}{dx}dx=2\pi h_0\int_{x_1}^{x_2}\frac{d}{dx}\left[\frac{1}{u}\right]dx=2\pi h_0\left[\frac{1}{u_2}-\frac{1}{u_1}\right]\ . \tag{11}$$

From (10) and (11) follows

$$p(x_1,x_2)\equiv\frac{L_{(x_1,x_2)}}{S(x_2-x_1)}$$
$$=-2\pi\frac{h_0}{(x_2-x_1)}\mathcal{R}\left[\frac{1}{u_2}-\frac{1}{u_1}\right]K\frac{dT}{dx}$$
$$=-H\left[\left[\frac{K}{u}\frac{dT}{dx}\right]_{x_2}-\left[\frac{K}{u}\frac{dT}{dx}\right]_{x_1}\right]$$
$$=H\left[\left[\frac{J_q}{u}\right]_{x_2}-\left[\frac{J_q}{u}\right]_{x_1}\right]$$
$$=H[(J_p)_{x_2}-(J_p)_{x_1}]\ , \tag{12a}$$

where $H\equiv2\pi(h_0/x_2-x_1)\mathcal{R}$. Generally, it will be

$$p(r_1,r_2)\mathbf{n}\equiv\frac{L_{(r_1,r_2)}}{S(r_2-r_1)}\mathbf{n}$$
$$=-H\left[\left[\frac{\mathsf{K}}{u}\cdot\mathrm{grad}T\right]_{r_2}-\left[\frac{\mathsf{K}}{u}\cdot\mathrm{grad}T\right]_{r_1}\right]$$
$$=H\left[\left[\frac{\mathbf{J}_q}{u}\right]_{r_2}-\left[\frac{\mathbf{J}_q}{u}\right]_{r_1}\right]$$
$$=H[(\mathbf{J}_p)_{r_2}-(\mathbf{J}_p)_{r_1}]\ , \tag{12b}$$

where $r=(x^2+y^2+z^2)^{1/2}$, $\mathbf{n}$ is the normal to section S oriented from r_1 to r_2. One can see that the pressure developed in the medium from r_1 to r_2 is proportional to the variation of the momentum flux in the same interval.

III. RADIATION FORCES PRODUCED BY ACOUSTIC WAVES ON A LIQUID-LIQUID INTERFACE AND ON A SOLID OBSTACLE SUSPENDED IN LIQUID

The pressure exerted by a sound wave on the interphase boundary between two immiscible liquids macroscopically at rest can be found from energetic considerations. As the two phases are to stay in mechanical equi-

librium, the "free"-energy density in one phase must be equal to the energy density in the other [35]. Of course, the mechanical equilibrium dealt with here is in the direction perpendicular to the interface and hence energy density of waves propagating at right angles to the interface should be considered. If the incidence angle of a wave is θ_1 and its (time averaged) energy density W_1, we decompose it into a perpendicular wave whose energy flux density equals $W_1 u_1 \cos\theta_1$ and a parallel wave of energy flux density $W_1 u_1 \sin\theta_1$. The expression $W_1 u_1 \cos\theta_1$ may be viewed as energy flux of a wave propagating at angle θ_1 whose energy density is $W_1 \cos\theta_1$. Assuming that the x axis is normal to the interface, the x component of this energy flux is $W_1 \cos\theta_1 u_1 \cos\theta_1$. Hence energy density of the component wave propagating perpendicularly to the interface with velocity u_1 is equal to $W_1 \cos^2\theta_1$. In the first liquid the reflected wave also propagates. The x component of that wave has energy density $W' \cos^2\theta_1$ by the same reasoning.

Thus the energy equation required at mechanical equilibrium has the form

$$W_1 \cos^2\theta_1 + W_1' \cos^2\theta_1 = W_2 \cos^2\theta_2 + p \ , \tag{13a}$$

where W_2 is energy density of the refracted wave, θ_2 the angle of refraction, and p the energy density due to pressure in the second liquid. Hence

$$p = (W_1 + W_1')\cos^2\theta_1 - W_2 \cos^2\theta_2 \ . \tag{13b}$$

In the case of normal incidence, it is easy to see that

$$p = 2W_1 \left[\frac{\rho_2 u_2 - \rho_1 u_1}{\rho_2 u_2 + \rho_1 u_1} \right]^2 , \tag{14}$$

where $\rho_1 u_1$ is the acoustic impedance in the first liquid and $\rho_2 u_2$ in the second.

Now we consider a liquid-solid interface, for instance, the front surface of a solid slab immersed in the liquid, kept in place by an external adjustable force. No pressure in the sense of free-energy density can be developed within the solid phase, nor can it develop in the liquid phase if the solid phase is just an obstacle suspended in the liquid. The same energetic criterion of mechanical equilibrium cannot be applied now; in order to calculate the pressure exerted by a sound wave impinging on a liquid-solid interface, we have to apply the momentum-balance equation, which we use here in the form of the Euler equation supplemented with the time-averaged momentum-flux-density tensor ($W n_i n_k$) due to the sound wave and the stress tensor S_{ik}. In the absence of external mass forces, we can write

$$\frac{\partial}{\partial t}\rho v_i = -\frac{\partial}{\partial x_k}(p\delta_{ik} + \rho v_i v_k + W_1 n_i^{(1)} n_k^{(1)} + W_1' n_i^{(1')} n_i^{(1')} + W_2 n_i^{(2)} n_k^{(2)} + S_{ik}) \ , \tag{15}$$

for the ith component of the momentum density, having adopted Einstein's convention on the sum. The symbol p here indicates the pressure of the fluid in motion, defined by a suitable equation of state; δ_{ik} is the Kronecker delta function. Indicating with π_{ik} the quantity in large parentheses and upon integration over a volume V, surrounded by surface S, we have

$$\frac{\partial}{\partial t}\int_V \rho v_i dV = -\int_V \frac{\partial}{\partial x_k}\pi_{ik} dV = -\int_S \pi_{ik} n_k dS \ , \tag{16}$$

with the use of Gauss's law. Thus the balance equation has the form

$$\frac{\partial}{\partial t}\int_V \rho v_i dV = -\int_S (p\delta_{ik} + \rho v_i v_k + W_1 n_i^{(1)} n_k^{(1)} + W_1' n_i^{(1')} n_k^{(1')} + W_2 n_i^{(2)} n_k^{(2)} + S_{ik}) n_k dS \ . \tag{17}$$

In a steady-state condition, neglecting infinitesimals higher than first order in v, we integrate over the liquid-solid interface which we assume to be of thickness δ (see Fig. 2).

For unit surface of the interface and the assumed situation of no movement of either phase and noting that no stress can develop at 0, the result of the integration along x normal to the interface is

$$\mathbf{S}_x(\delta) = \mathbf{k}_x [W_2 \cos^2\theta_2 - (W_1 + W_1')\cos^2\theta_1] \ , \tag{18a}$$

having set $S_i \equiv S_{ik} n_k$ and $\mathbf{k}_x$ being a unit vector along x. Without reflection and for perpendicular incidence this gives us

$$\mathbf{S}_x(\delta) = \mathbf{k}_x (W_2 - W_1) \ . \tag{18b}$$

Now we calculate the mechanical effect on a solid-liquid interface, assuming the solid and the liquid to be the same as previously and with no reflection (see Fig. 3). Since no stress can develop at δ, the result of the integration is

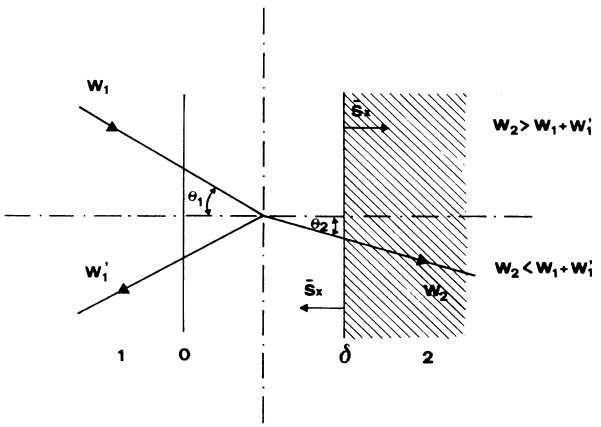

FIG. 2. Liquid-solid interface of thickness δ. Incident, reflected and refracted waves of respective energy densities W_1, W_1', and W_2 for angle of incidence θ_1 generate stress vector S_x in the solid, pointing right (upper part of figure), or left (lower part) depending on the condition $W_2 \gtrless W_1 + W_1'$.

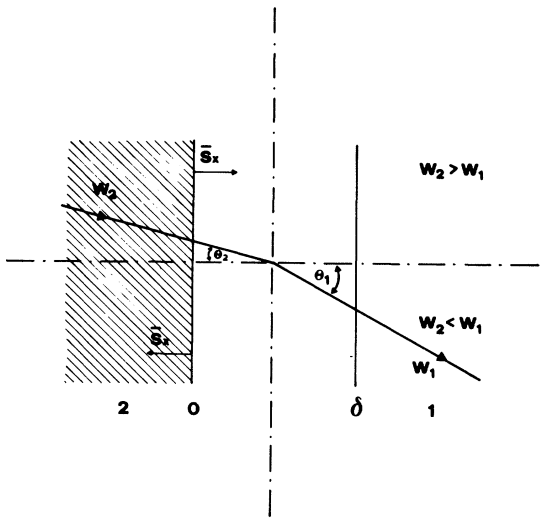

FIG. 3. Solid-liquid interface of thickness δ; as above, but with no reflection. The upper part shows stress vector in the solid in the case $W_2 < W_1$; the lower part refers to the case when $W_2 > W_1$.

$$\mathbf{S}_x(0)=\mathbf{k}_x(W_2\cos^2\theta_2 - W_1\cos^2\theta_1) . \tag{19a}$$

Hence for perpendicular incidence, we have

$$\mathbf{S}_x(0)=\mathbf{k}_x(W_2 - W_1) . \tag{19b}$$

Having obtained the same result as for liquid-solid interfaces, we finally obtain for the stress vector at both interfaces the expression

$$p\mathbf{k}_x=\mathbf{S}_x(\delta)+\mathbf{S}_x(0)=2\mathbf{k}_x(W_2 - W_1) , \tag{20}$$

representing a pressure proportional to the difference of acoustic energy density in the media. In the case, considered by us, of a solid slab kept in place by an external adjustable force $\mathbf{f}^{\text{ext}}$, the nonzero resultant stress can be identified with that force, so that $p\mathbf{k}_x + \mathbf{f}^{\text{ext}}=0$. Equation (20) can be experimentally checked by measuring $\mathbf{f}^{\text{ext}}$, which gives us access to "radiation force."

IV. THERMAL-RADIATION FORCES IN NONISOTHERMAL SYSTEMS

A. Thermal-radiation forces on a solid slab

In the case of heat flow the momentum-flux tensor coupled to heat flux has the form $(J_q n_i n_k)/u$, because in this case the energy density $W=J_q/u$.

Expression (20) for radiation pressure of acoustic waves on a solid slab may be tentatively written, in the case of a flux of thermal excitations, in the form

$$p=2H^*\left[\frac{J_q^A}{u_A}-\frac{J_q^B}{u_B}\right] , \tag{21}$$

where the slab has been situated horizontally and A stands for the liquid phase and B for the slab. The logical gap between Eqs. (12) and (20) may be bridged by bringing sections x_1 and x_2 progressively nearer to one another, leaving the temperature difference $(T_1 - T_2)$ constant. We thus have in the limit a surface of discontinuity, between warm and cold liquid, the form of Eq. (12) remaining unchanged, i.e., the pressure p staying proportional to the difference of momentum-flux densities. The numerical proportionality constant however may be different from H since this constant depends on the average properties between x_1 and x_2, while in the present case only the "local" conditions at the discontinuity are involved; we shall call it H^*, without discussing for the time being the problem in more detail. Now the difference in physical properties of the two materials in contact may also be generalized, including differences in composition or state, leaving unaltered the form of Eq. (12). We see that an expression analogous to Eq. (12) has been arrived at in a completely independent way, upon substitution in Eq. (20) of energy density due to heat flow in place of acoustic energy density.

Making use of Fourier's law and introducing the slab surface σ_p, Eq. (21) allows us to write the following expression for the thermal-radiation force on a slab or plunger suspended in a liquid:

$$F_{\text{slab}}^{\text{th}}=2\sigma_p H^*\left[\left[\frac{K}{u}\frac{\Delta T}{\Delta x}\right]_A - \left[\frac{K}{u}\frac{\Delta T}{\Delta x}\right]_B\right] . \tag{22}$$

The subscripts A and B mean that the values of the quantities concerned are those of phase A and B, respectively. The material constants K and u depend on temperature. Equation (22) neglects that dependence and takes the respective quantities at the average temperature $T_{\text{av}}=-(T_1'+T_2')/2$. A more exact formula is

$$F_{\text{slab}}^{\text{the}}=\sigma_p H^*\left\{\left[\left[\frac{K}{u}\frac{\Delta T}{\Delta x}\right]_A - \left[\frac{K}{u}\frac{\Delta T}{\Delta x}\right]_B\right]_{T_1'} - \left[\left[\frac{K}{u}\frac{\Delta T}{\Delta x}\right]_B - \left[\frac{K}{u}\frac{\Delta T}{\Delta x}\right]_A\right]_{T_2'}\right\} . \tag{23}$$

When the solid slab is very thin and/or the temperature gradient is not too steep, Eq. (22) is a good enough approximation and will be used here for calculations as well as for qualitative discussions. Thus whenever the energy density J_q/u due to heat flow in a solid slab B suspended in a liquid A is greater than that in the liquid, the force acting on the slab is counter to the heat flow; and instead it has the sense of the heat flux, when the energy density of the slab is smaller than that of the liquid. As the heat-flow coupled energy density $J_q/u=(K/u)(\Delta T/\Delta x)$ is equal to the absolute value of the heat-flow coupled momentum flux, one can also loosely say that solid material with thermal momentum conductivity K/u greater than that of the liquid is pushed counter to the heat flux; the push will be in the sense of the heat flux in the opposite case. This is a clear-cut prediction of the theory, readily amenable to experimental verification.

B. Thermal-radiation forces on solute particles

Equation (22) could be applied in principle to objects of any size suspended in a nonisothermal liquid; its extrapolation to ionic or molecular solute particles requires some caution however. Momentum should be transferred at different rates to solute and solvent particles to generate nonvanishing time-averaged effects on solution components. On the other hand the impinging phonons might be unable to discriminate among objects having diametral dimensions comparable with their own wavelength. Stating the problem in a different form, it can be questioned whether the expression $(K/u)(dT/dx)$ can be defined with reference to a single ion or molecule. Another independent problem concerns the possible contribution of side forces, not accounted for in the homogeneous-phase system treated above. In the case of flat, thin disks having a large cross section normal to the heat flux, the approximation is acceptable. Thus thermal-radiation force on a flat, thin disk will be practically coincident with the "front force" given by Eq. (22) but obviously this argument cannot be extended to objects as small as a solute particle.

The development of an exact theory of phonon-particle interactions is laden with difficulties, and it seems thus preferable to follow an alternative procedure. We shall express the phenomenological coefficients of thermal diffusion in terms of thermal-radiation forces, and then compare experimental results with these expressions. It is expected that the comparison will yield some clear-cut evidence lending support to the assumption that thermal-radiation forces are the physical cause of thermodiffusive effects in solutions. At the same time by comparing theoretical expressions with the actual phenomenology, one could also obtain hints on the kind of refinements needed to construct a more appropriate theory for the calculation of momentum exchanges among phonon excitations and solution components. It is easy to derive the expressions for thermodiffusive phenomenological coefficients within the frame of reference of Eq. (22). Applying this equation to a solvated solute particle of radius r_0 one gets for the net thermal-radiation force $F_p^{\rm th}$ acting on it the value

$$(F_p)^{\rm th}=2\pi r_p^2 H^* \left[\left[\frac{K}{u} \right]_l - \left[\frac{K}{u} \right]_p \right] \left\langle \frac{dT}{dx} \right\rangle_x , \tag{24}$$

where subscripts p and l, respectively, indicate the solvated solute particle and the surrounding liquid. The distinction between the value of the temperature gradient in the particle and the surrounding liquid has been dropped in the second term where only the space-averaged temperature gradient $\langle dT/dx \rangle_x$ is considered. The introduction of the cross section πr_p^2 of the solvated particle in Eq. (24) is justified because the bound solute shall have a momentum conductivity different from the surrounding liquid. Accordingly the "object" different from the solution in bulk, is not the naked solute, but the entire solvated particle.

The force $F_p^{\rm th}$ will cause solute drift with a velocity $v_d=D'(dT/dx)$ where $D'(\mathrm{cm^2\,s^{-2}\,°C^{-1}})$ is the thermal diffusion coefficient of the particle, defined as drift velocity in a unitary temperature gradient. The value of v_d shall be determined by the power balance equation

$$W_p^{\rm th}=W_p^{\eta} , \tag{25}$$

stating the equality of the power input $W_p^{\rm th}$ due to the work performed by thermal-radiation forces and the energy dissipated per second by the particle through hydrodynamic friction W_p^{η}. In ordinary thermal diffusion the center of mass of the liquid is stationary, and with dilute solutions, solvent backflow can be neglected, thus solute motion occurs in a standing liquid and the power balance equation reduces to the balance of thermal-radiation force and viscous drag, the latter being given by the Stokes equation. Assuming solvated solute particles to be spherical

$$D'=H^*\frac{r_p}{3\eta_l}\left[\left[\frac{K}{u} \right]_l - \left[\frac{K}{u} \right]_p \right] , \tag{26}$$

η_l being the viscosity of the solution. From Eq. (26) it is immediate to deduce the expression for Soret coefficient $s=D'/D$ $(°\mathrm{C^{-1}})$, where D $(\mathrm{cm^2\,s^{-1}})$ is the coefficient of isothermal diffusion. Making use of the Stokes-Einstein equation to eliminate the product $\eta_l D$ we get

$$s=H^*\frac{2\pi r_p^2}{k_B T_{\rm av}}\left[\left[\frac{K}{u} \right]_l - \left[\frac{K}{u} \right]_p \right] , \tag{27}$$

where k_B is Boltzmann constant and $T_{\rm av}$ is the average solution temperature.

Since the concentration ratio in the cold and warm solution at thermodiffusive steady state is $C_C/C_W=\exp s\Delta T$, one also has

$$\frac{C_C}{C_W}=\exp\left\{ H^*\frac{2\pi r_p^2 \Delta T}{k_B T_{\rm av}}\left[\left[\frac{K}{u} \right]_l - \left[\frac{K}{u} \right]_p \right] \right\} . \tag{28}$$

This concentration ratio is reached at steady state in a gravitationally stable nonisothermal solution, when thermodiffusive solute flux and diffusive counter-flow balance each other, i.e., when the temperature gradient is in equilibrium with the gradient of the chemical potential.

Due to the approximations introduced in our treatment, expressions (26)–(28) are not expected to be quantitatively accurate but should allow clear-cut qualitative and semiquantitative predictions on the phenomenology of thermal diffusion in the condensed phases.

A qualitative prediction is that upon change of sign of the quantity $(K/u)_l-(K/u)_p$ an inversion should occur in the sense of solute thermodiffusive drift relative to the temperature gradient. Two semiquantitative predictions are as follows.

(1) That the value of the Soret coefficient of quasispherical macromolecular solutes should be proportional to r_p^2 and hence that a series of molecular cuts of polymer should exhibit a dependence of s on molecular mass M, given by $s=AM^{2/3}$.

(2) That the experimental values of D', s, and C_C/C_W should lead, through Eqs. (26)–(28) to values of $(K/u)_l-(K/u)_p$ consistent with those derived from the

ratios of thermal conductivities and velocities of propagation of elastic waves of the respective materials in bulk.

V. EXPERIMENTAL MEASUREMENT OF THERMAL-RADIATION FORCES

If the concept of thermal-radiation force is valid, many aspects of the phenomenology of nonisothermal systems will have to be reconsidered. Here however, in view of the preliminary character of this paper, we attempt only to check experimentally the four fundamental predictions of the theory, namely, in the first place that measurable forces should be produced by heat flux on solid-liquid and liquid-solid interfaces as well as on molecular "obstacles" and even in liquid mixtures; second that such forces should be proportional to the temperature gradient; third that the intensity and the sense of the measured forces should depend on the nature of the two adjacent media and on their order of succession along the temperature gradient; finally that the forces should depend on the average temperature as the momentum conductivities of the components.

The experimental system employed is the following: a solid slab B is immersed in a nonisothermal liquid so that thermal-radiation forces are expected to act on the slab. Of course, the plungers have side walls, where forces distinct from those discussed above might appear in the nonisothermal condition. Still, if the plunger is cut in the form of a flat, thin disk, the forces on the lateral surface can be neglected. According to Eq. (22), we assume thermal-radiation force on the plunger to be given by

$$F^{\text{th}}_{\text{Plunger}} = 2\sigma_p H^* \left[\left[\frac{K}{u} \frac{\Delta T}{\Delta x} \right]_l - \left[\frac{K}{u} \frac{\Delta T}{\Delta x} \right]_s \right], \quad (29)$$

subscripts l and s indicating "liquid" and "solid," respectively, and σ_p being the plunger's cross section normal to x. Values of K and u must be taken at the average temperature $T_{\text{av}} = (T'_1 + T'_2)/2$.

The force acting on the plunger will displace it, unless an equal and opposite force is applied from outside. This force can be easily supplied and measured by means of the apparatus schematically described in Fig. 4. The solid shaped as a flat disk, immersed in the liquid contained in the cell, hangs on the arm of a balance. The upper and lower metallic surfaces of the cell can be, respectively, heated and cooled, the lateral walls are of a thermal insulating material.

It should be mentioned here that we already derived some time ago, from dimensional considerations, an expression very similar to Eq. (29) for the thermal-radiation force acting on a solid slab [13,14]. We then provisionally expressed the constant of thermal-radiation force by means of the transmission coefficient of acoustic waves. Preliminary experiments with a variety of solids and liquids were performed and have been described by us elsewhere [14,17]. Presently, in view of the fundamental importance of these measurements as a direct check of the theory of thermal-radiation forces, we have performed the additional series of experiments described here, employing an improved version of the apparatus and covering a wider choice of system composition and of physical parameters.

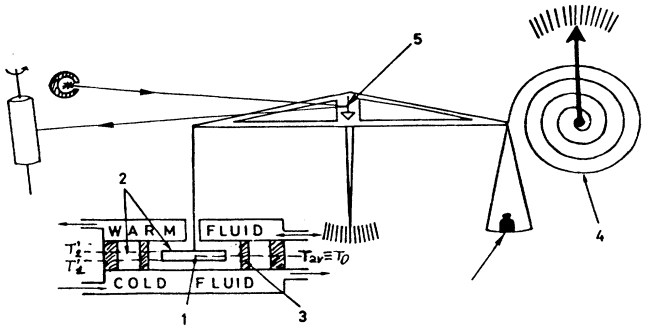

FIG. 4. Schematic representation of our apparatus. Plunger (1) is accurately counterbalanced at temperature T_0: then the upper flow chamber is heated to T_2 and the lower flow chamber cooled to T_1 subject to the condition $T_0 \equiv T_{\text{av}} = (T_1 + T_2)/2$. Heat flows through the liquid (2) and the plunger. The guard ring (3) prevents convective disturbances. Thermal-radiation force is compensated by means of dynamometric measuring device (4). Plunger movement can be detected by optical device (5) to better than ± 0.005 cm.

In the conditions of Fig. 4 heat will flow through liquid and the plunger, the fluid being gravitationally stable. The cylindrical guard ring ensures protection from convective disturbances eventually originating at the cell wall. The force exerted by the plunger on the balance arm is accurately counterbalanced at the initial temperature T_0 by weights placed in the balance dish. In this condition the dynamometric device exerts no force. The temperature gradient is applied subject to the condition that the temperature at the plunger's midheight $T_{\text{av}} \equiv T_0$. The forces produced by the heat flux on the plunger are measured at the dynamometric device. In the previous measurements, the balance deflection was used to determine the force acting on the plunger, which consequently was allowed to change slightly its position during measurement, and this resulted in a small variation of average temperature and of buoyancy forces. In the present measurements the plunger position was kept fixed, by applying a continuously controllable force to the balance arm, by means of the dynamometer; this force measures the thermal-radiation force acting on the plunger. It is required that the solid slab is very thin and that the temperature $T_{\text{av}} \equiv T_0$ at the level of the slab stays constant during measurement. Complete absence of convection must be ensured, this last condition being easily checked: the light beam reflected by a mirror attached to the balance is focused on a sliding film and photographically recorded. In this way the eventual occurrence of convection in the cell is readily detected by oscillations on the trace of the film. Temperature at various levels in the cell was continuously measured by means of thermistors suitably positioned, their output being registered on a twelve channel Leeds and Northrup Speedomax recorder. Measured forces are generally found to increase with time until a constant maximum value is reached—in coincidence with attainment of the steady-state temperature distribu-

tion in the cell, as revealed by the thermocouples.

One series of measurements was carried out at the initial temperature T_0 coincident with final average temperature $T_{av} = +15\,°C$ employing various solids and liquids. The plungers were kept at the cell's middle height; all plungers were 0.15 cm thick and of circular cross-sectional area $\sigma_p = 7.068\ cm^2$. The temperature gradient was 30 °C/cm ($\Delta T = 21\,°C$; cell height $h = 0.7$ cm). Results of these measurements are reported in Table I, where the measured forces are also compared with ex-

TABLE I. Calculated and measured thermal-radiation forces on plungers 0.15 cm thick, having a cross section of $\sigma_p = 7.068\ cm^2$, when the applied temperature gradient is $dT/dx = 30\,°C/cm$ and average temperature $T_{av} = 15\,°C$. Theoretically expected values calculated from Eq. (29) as explained in the text. Forces directed against the sense in which heat flows are marked with a minus sign. All experimental data are average values relative to four distinct experiments conducted in identical conditions, with the exception of those marked a, where the plunger was slightly affected by exposure to solvent. No systematic effect on successive measurements was detected in these cases.

System	$\left[\frac{k_{yy}}{u}\right]_l - \left[\frac{K_{yy}}{u}\right]_s$ (dyn cm^{-1} K^{-1})	Thermal-radiation force: Expected (dyn)	Thermal-radiation force: Measured (dyn)	(Measured force)/(Expected force) (%)	Observations
Water-polyethylene	0.264	111.95	85.06	76	First sample
Water-polyethylene	0.267	113.20	88.25	78	Second sample
Water-Plexiglas	0.342	144.08	87.82	61	
Water-glass (Crown)	0.325	137.88	112.71	82	
Water-nylon 6-6	0.308	130.80	114.94	88	
Water-rubber (Ebonite)	0.382	161.99	141.00	87	
Methanol-polyethylene	0.0405	17.17	11.16	65	First sample[a]
Methanol-polyethylene	0.0476	20.19	13.53	67	Second sample[a]
Methanol-nylon 6-6	0.0770	32.74	21.60	66	
Methanol-glass (Crown)	0.1085	46.01	30.83	67	
Ethanol-polyethylene	0.0036	1.52	undetectable		First sample[b]
Ethanol-polyethylene	0.0105	4.47	3.28	72	Second sample[b]
Ethanol-glass (Crown)	0.0716	30.38	22.20	73	Second sample[b]
Ethanol-Plexiglass	0.0862	36.55	27.04	74	
Ethanol-nylon 6-6	0.0403	17.09	14.70	86	
Butanol-polyethylene	−0.0205	−8.69	−7.38	85	First sample
Butanol-polyethylene	−0.0136	−5.77	−4.97	86	Second sample
Butanol-glass (Crown)	0.0475	20.14	18.33	91	
Isopropyl-polyethylene	−0.0270	−11.39	−10.25	90	First sample
Isopropyl-polyethylene	−0.0195	−8.29	−7.21	87	First sample
Isopropyl-glass (Crown)	0.0409	17.37	14.76	85	
Isopropyl-nylon 6-6	0.0096	4.07	3.84	94	
Isopropyl-Plexiglas	0.0555	23.54	20.72	88	
n-Heptane-polyethylene	−0.0198	−8.40	−6.87	82	First sample
n-Heptane-polyethylene	−0.0129	−5.48	−4.11	75	Second sample
n-Heptane-Plexiglas	0.0626	26.27	17.84	67	
n-Heptane-nylon 6-6	0.0167	7.10	6.24	88	
n-Heptane-glass (Crown)	0.0481	20.40	18.27	89	
Carbon tetrachloride-Plexiglas	0.0531	22.50	15.75	70	
Carbon tetrachloride-nylon 6-6	0.0071	2.33	≃2	≃85	
Carbon tetrachloride-glass (Crown)	0.0385	16.32	13.16	81	
Ortoxylene-polyethylene	−0.0431	−18.28	−15.72	86	First sample
Ortoxylene-polyethylene	−0.0362	−15.35	−13.51	87	Second sample
Ortoxylene-Plexiglas	0.0395	16.75	13.20	79	
Ortoxylene-glass (Crown)	0.0250	10.60	9.33	88	

[a]Plunger's surface was slightly affected by interaction with solvent. Effect on measured force was negligible as shown by repeated measurements.

[b]Expected values have been calculated from parameters relative to pure ethanol; actual measurements however were conducted without protection from ambient air.

pected values, calculated from Eq. (29). In the calculation of the force the group velocity u at ultrasonic frequencies has been used in place of the phase velocity of hyperfrequency thermal waves, which is unknown. Other measurements were performed to check the dependence of the force acting on the plunger from the average temperature and from the temperature gradient; some of these results are summarized in Tables II and III.

For the reader's convenience in Fig. 5 the K/u ratios of the materials presented in Tables I–III are plotted in graphical form against temperature. The values of K and u for these substances have been found in the literature. Solid lines are used for liquids, dashed lines for the solid samples actually used by us in the present study. Measurements of K and u of these samples have been performed in our laboratory as described below.

As can be seen from Tables I–III the measured values of the radiation forces are found to exhibit all the qualitative features predicted by the theory; furthermore, the quantitative agreement is rather good, since experimental results average at about 80% of theoretical values. Sign reversal of the measured force relative to the sense of the temperature gradients always takes place as predicted. Substitution of water, with methyl, or ethyl, butyl, isopropyl alcohol produces a variation in the measured radiation force consistent with the respective momentum conductivities of these liquids. The proportionality of measured forces to the intensity of the applied temperature gradient clearly emerges from inspection of experimental results. The temperature dependence of the effect in turn is consistent with the temperature dependence of the differences of the K/u of each pair of substances employed. From Table II this fairly good agreement between expected and measured forces at various (average)

TABLE II. Thermal-radiation forces calculated from Eq. (29) and actually measured at constant temperature gradient $dT/dx = 30\,°C/cm$ and various average temperatures. Cell height and dimension of solid plungers in these experiments were the same as above.

System	T_{av} (°C)	Thermal-radiation force: Expected (dyn)	Thermal-radiation force: Measured (dyn)	(Measured force)/(Expected force) (%)	Observations
Water-polyethylene	15	111.95	85.06	76	First sample
Water-polytehylene	25	112.20	86.51	77	First sample
Water-polyethylene	27	112.60	86.43	77	First sample
Water-polyethylene	30	113.35	86.00	76	First sample
Water-polyethylene	47	116.62	88.42	76	First sample
Water-polyethylene	15	118.67	92.00	77	Second sample
Water-polyethylene	25	113.20	88.25	78	Second sample
Water-polyethylene	27	109.41	85.32	78	Second sample
Water-polyethylene	35	102.08	79.20	77	Second sample
Ethanol-polyethylene	7	0.00	undetectable		First sample
Ethanol-polyethylene	15	1.52	undetectable		First sample
Ethanol-polyethylene	26	3.09	2.2	71	First sample
Ethanol-polyethylene	45	8.10	7.5	92	First sample
Ethanol-polyethylene	7	8.48	5.76	68	Second sample
Ethanol-polyethylene	15	4.47	3.28	72	Second sample
Ethanol-polyethylene	26	0.46	undetectable		Second sample
Ethanol-polyethylene	45	−13.61	−9.79	72	Second sample
Water-glass (Crown)	15	137.88	112.71	82	
Water-glass (Crown)	27	139.90	111.92	80	
Water-glass (Crown)	47	142.03	114.28	80	
Isopropanol-polyethylene	15	−11.39	−10.25	90	First sample
Isopropanol-polyethylene	26	−9.12	−7.38	81	First sample
Isopropanol-polyethylene	30	−7.89	−5.99	76	First sample
Isopropanol-polyethylene	15	−8.29	−7.21	87	Second sample
Isopropanol-polyethylene	27	−11.75	−9.42	80	Second sample
Carbon tetrachloride-nylon 6-6	7	2.84	2.30	81	
Carbon tetrachloride-nylon 6-6	15	2.33	~2	~85	
Carbon tetrachloride-nylon 6-6	26	1.65	undetectable		
Carbon tetrachloride-nylon 6-6	45	−2.76	−2.05	74	

TABLE III. Thermal-radiation forces calculated and measured at the constant average temperature $T_{av}=27\,°C$ and with various intensities of the applied temperature gradient. In the case of the system (carbon tetrachloride nylon 6-6) average temperature was $+45\,°C$.

System	$\frac{dT}{dy}$ (°C cm^{-1})	Thermal-radiation force Expected (dyn)	Measured (dyn)	(Measured force)/(Expected force) (%)	Observations
Water-polyethylene	10	37.53	28.13	75	First sample
Water-polyethylene	20	75.06	54.04	72	First sample
Water-polyethylene	30	112.60	86.43	77	First sample
Water-polyethylene	35	131.36	86.65	78	First sample
Water-glass (Crown)	10	46.63	36.36	78	
Water-glass (Crown)	20	93.26	76.47	82	
Water-glass (Crown)	30	139.90	111.92	80	
Water-glass (Crown)	35	163.21	133.82	82	
Isopropanol-polyethylene	10	−3.92	−3.17	81	Second sample
Isopropanol-polyethylene	30	−11.75	−9.42	80	Second sample
Isopropanol-polyethylene	35	−13.70	−11.37	83	Second sample
Carbon tetrachloride-nylon 6-6	20	−1.84	−1.47	80	$T_{av}=+45\,°C$
Carbon tetrachloride-nylon 6-6	30	−2.76	−2.05	74	$T_{av}=+45\,°C$

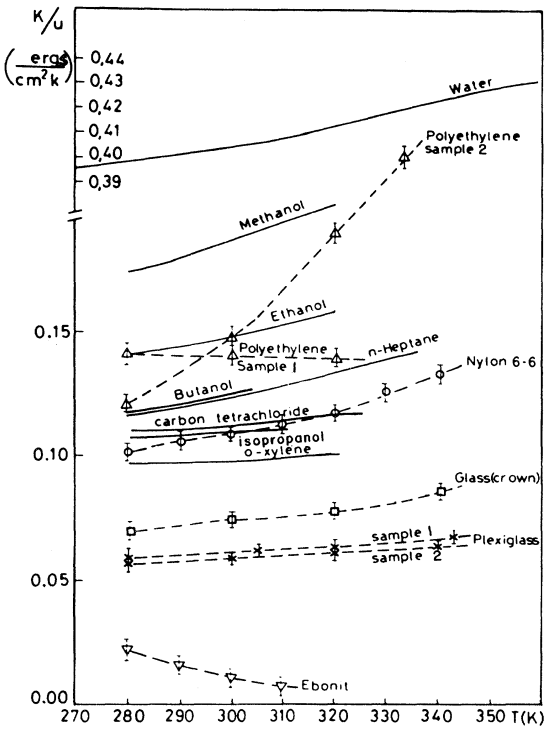

FIG. 5. The momentum conductivities of liquids and solids composing the systems in which thermal-radiation forces have been measured in this study are plotted against temperature. Liquids: solid lines—data from the literature. Solids: dashed lines—our own measurements. Each of these last points is the average of three measurements, the corresponding fiducial limits are indicated.

temperatures can be appreciated.

In reading Tables I–III one should remember that "expected values" have been calculated from Eq. (29): solvent momentum conductivities being derived from the handbook data as explained above, while the momentum conductivities of the plungers have been obtained by direct measurements of K and u on each sample at various temperatures. These measurements were performed by a thermoconductometer (Colora of Messtechnik GMBH) and by an ultrasonic interferometer, using standard procedures.

We shall proceed now to discuss experimental evidence on the thermodiffusive behavior of various kinds of solutions. For this it was not necessary to do measurements *ad hoc* in view of the existence of a great number of published experimental works on the Soret effect in liquid mixtures. This evidence shall be discussed here with reference to our theoretical approach.

(1) *Coincidence of inversions in the sense of thermodiffusive solute drift with the change of sign of the expression* $(K/u)_l-(K/u)_p$. Studies of thermodiffusive behavior of solutions of polyvinylpyrrolidone $K90$ of 360 000 amu in the solvents water, methanol, ethanol, *n*-butanol, and isopropanol, evidenced an inversion in the sense of solute drift among the first three and the last two of these solvents [17]. This is precisely what would be expected on the basis of the comparison of the k/u value of the solute with the ones of the solvents, as shown in Table IV.

(2) *Dependence of the value of Soret coefficient on the molecular mass of a polymeric solute.* Accurate measurements of the value of the Soret coefficient as a function of the molecular weight of a polymeric solute were performed by Emery and Drickamer [36] using various cuts of polystyrene in toluene. The molecular weights of the

TABLE IV. Soret coefficients, measured in solutions of polyvinylpyrrolidone $K90$ (360 000 amu) in various solvents are compared with differences of the K/u ratios. Change of sign of s and of $(K/u)_l-(K/u)_p$ occurs in n-butanol and isopropanol relative to the first three solvents which have higher $(K/u)_l$ values.

Solution	$\left[\frac{K}{u}\right]_l$ $\left[\frac{\text{erg}}{\text{cm}^2\,^\circ\text{C}}\right]$	$\left[\frac{K}{u}\right]_p$ $\left[\frac{\text{erg}}{\text{cm}^2\,^\circ\text{C}}\right]$	$\left[\left[\frac{K}{u}\right]_l-\left[\frac{K}{u}\right]_p\right]$ $\left[\frac{\text{erg}}{\text{cm}^2\,^\circ\text{C}}\right]$	$S=\frac{D'}{D}(^\circ\text{C}^{-1})$
Polyvinylpyrrolidone $K90$ in water	0.4031	0.137	0.266	19.82×10^{-3}
Polyvinylpyrrolidone $K90$ in methanol	0.1830	0.137	0.046	0.38×10^{-3}
Polyvinylpyrrolidone $K90$ in ethanol	0.1440	0.137	0.007	2.31×10^{-3}
Polyvinylpyrrolidone $K90$ in butanol	0.1205	0.137	−0.016	-5.78×10^{-3}
Polyvinylpyrrolidone $K90$ in propanol	0.1197	0.137	−0.017	-6.01×10^{-3}

solute ranged from 1×10^4 to 338×10^5 amu. The experimental points fit very nicely a curve drawn for the function $s=AM^{2/3}$, where the value of the constant A has been obtained by fitting the expression to the central experimental point of the series (Fig. 6). Other data confirming this law of dependence on the solute mass have been published by Debye and Bueche [37], Langhammer [38–41] and by ourselves [18].

(3) *Comparison of the values of the K/u ratios determined by experiments of thermal diffusion with those obtained by independent methods.* The ratios of thermal conductivity and velocity of propagation of elastic waves in solids and liquids can be calculated directly from the tabulated values of these two quantities. Obviously these data refer to materials in bulk, not to their isolated costituent particles. Experimentally measured orders of magnitude of s are found to range between zero and $10^{-3}\,^\circ\text{C}^{-1}$ for small particles and up to $10^{-2}\,^\circ\text{C}^{-1}$ for larger molecules; those of D' range between zero and $10^{-7}\ \text{cm}^{-2}\,\text{s}^{-1}\,^\circ\text{C}^{-1}$ for small solutes and are as high as $10^{-6}\ \text{cm}^2\,\text{s}^{-1}\,^\circ\text{C}^{-1}$ in the case of macromolecules [18]. From these experimental values the $(K/u)_p$ can be calculated by means of Eqs. (26)–(28) in which the values of $(K/u)_l$ for the solvent in bulk are introduced; then the $(K/u)_p$ turns out to be comparable with those of the corresponding materials in bulk. It appears therefore evident that it is not nonsensical to consider the ratio of K/u as a quantity which can be defined also with reference to a single solute particle.

(4) *Temperature dependence of Soret coefficient in benzene and n-heptane mixtures.* Bierlein, Finch, and Bowers [42] have studied thermal diffusion in mixtures containing various amounts of benzene in n-heptane, namely 20%, 40%, 50%, by weight. In every case when the average temperature of the solutions was varied from $+18\,^\circ\text{C}$ to over $+60\,^\circ\text{C}$, Soret coefficients were found to decrease, pass through zero and then increase with an inverted sign. Sign inversion of s occurred at about $+57\,^\circ\text{C}$ in solutions containing less then 50% benzene and at about $+60\,^\circ\text{C}$ in those with over 50% benzene.

Interestingly, the temperature dependence of the K/u ratios of benzene and toulene in bulk is such that also the difference $(K/u)_{\text{benzene}}-(K/u)_{n\text{-heptane}}$ changes sign at about $+57\,^\circ\text{C}$, being equal to zero at that temperature.

The value of these ratios for the two substances in bulk are plotted against temperature in Fig. 7. The values of the Soret coefficient for benzene in the three mixtures containing not over 50% benzene are plotted against temperature in Fig. 8. The coincidence of the temperature where no thermal diffusion occurs ($s=0$) with the

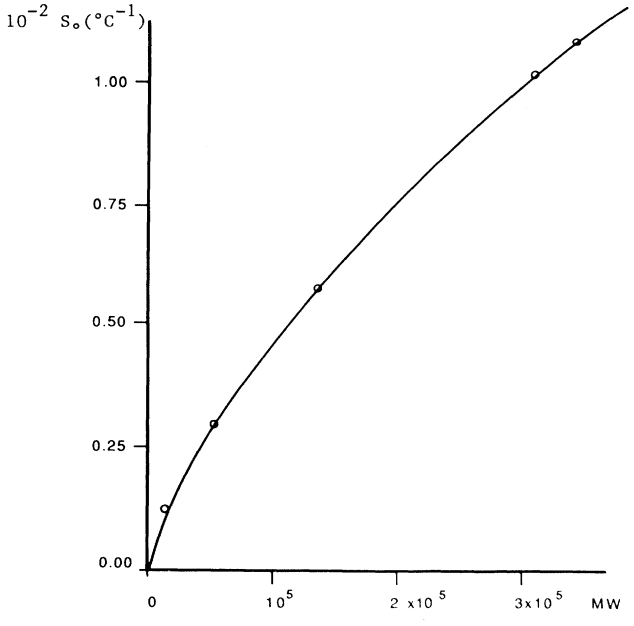

FIG. 6. Experimental values of the Soret coefficient for various cuts of polystyrene molecules in toluene, obtained by Emery and Drickamer (circles). The solid curve drawn through the third experimental point represents the function: $s=HM^{2/3}$.

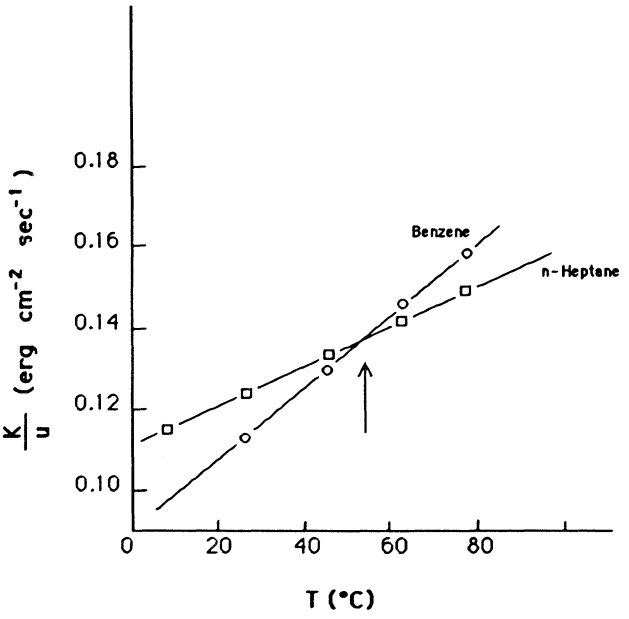

FIG. 7. Momentum conductivities of benzene (○) and *n*-heptane (□) are plotted against temperature. The two plots intersect at $T = +57\,°C$, a temperature where the difference of the K/u ratios vanishes.

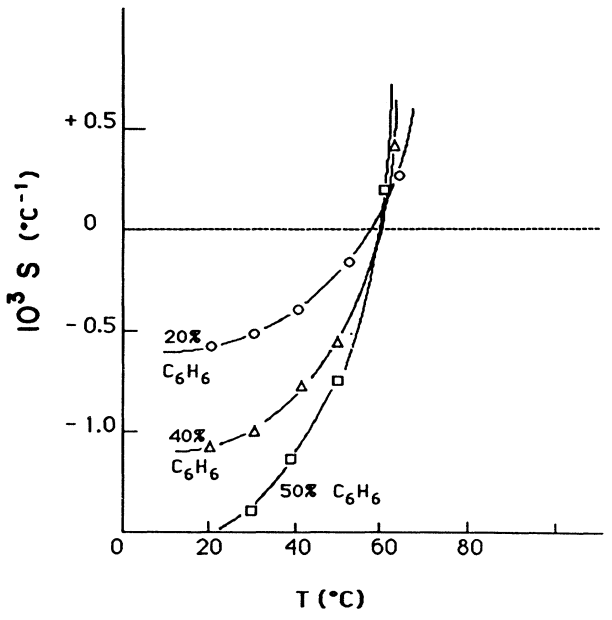

FIG. 8. Values of Soret coefficients of benzene in mixtures with *n*-heptane, measured at various average temperatures. The results plotted in the figure have been obtained in solutions containing respectively 20 mol% (●); 40 mol% (▲) and 50 mol% (■) in weight of C_6H_6. In each case the sense of thermodiffusive drift inverts at the (average) temperature $T_{av} = +57\,°C$. The inversion point occurs where the Soret coefficient goes through the value $s = 0$.

one where the difference of the K/u of the components vanishes is striking as well as is the inversion in the sense of thermodiffusive drift below and above that point.

The straightforward interpretation of these results clearly is that in the case of two weakly interacting substances, such as benzene and *n*-heptane, each molecule of either component exhibits the K/u of the respective substance in bulk. Phonon-particle interactions thus appear to be events leading to momentum transfer and to the production of radiation pressure in accordance with our theory, even on obstacles having diametral dimensions comparable with phonon wavelengths.

VI. DISCUSSION AND CONCLUSIONS

A critical survey of the experiments described in Sec. V will be useful, particularly for those with the solid disks since, notwithstanding their great conceptual simplicity, the interpretation of results requires much care to avoid the interference of unwanted effects and ensure that the measured forces are due only to thermal-radiation effects. Two major causes of error reside in the possible appearance of convective motions in the liquid and in uncompensated buoyancy effects on solid slabs, having the thermal-expansion coefficient different from the liquid one. A third possible source of error could reside in unaccounted surface tension forces acting on the suspension wire, where it emerges from the liquid surface.

The first difficulty was overcome by careful alignment of heating and cooling metallic surfaces in horizontal planes, and by introducing a coaxial cylindrical guard ring around the cylindrical slab, as shown in Fig. 4. We also found that—for reasons which are not clear to us—cooling from below for some 20 min before heating from above greatly decreased the probability of convection. Whenever notwithstanding these precautions some turbulent motion was produced, it was readily detected by the optical device used to read the position of the balance arm.

Much more difficult is the problem set by thermal expansion. It is easily seen that differential thermal expansion of liquid and solid may produce effects having the same order of magnitude of thermal-radiation forces. To avoid interference of buoyancy effects we took care to ensure that the temperature at midheight of the solid plunger was the same at steady-state temperature distribution and in the initial uniform temperature state. A series of thermocouples were radially inserted in the chamber containing the nonisothermal liquid, at various heights, one of them right at the level of the midsection of the plunger. Only when steady-state temperature distribution was achieved and temperature at the plunger's level was back to initial value the measured force was assumed to correspond to net thermal-radiation force.

Under these conditions a slight modification ($\Delta T = \pm 0.2\,°C$), deliberately induced in the temperature of one of the thermostats controlling the temperature gradient—a change this time that produced a temperature variation of $\Delta T = \pm 0.1\,°C$ at the central thermocouple—resulted in a barely detectable variation of 1–2 % of the force measured at the dynamometer.

This effect, which operatively defines the sensibility and precision of our apparatus, was found to be due much more to the variation produced in the temperature gradient than to effects due to the variation of buoyancy. We could ascertain this circumstance by selectively playing on average temperature and/or on the temperature gradient respectively. For instance, simultaneous opposite changes of 0.1 °C in the temperature of the two thermostats (affecting grad$T$ but not T_{av}) altered the measured force more than simultaneous changes of ± 0.2 °C in the same sense of both temperatures.

The third possible source of systematic error is easily disposed of. The suspension wire is only 0.1 mm in diameter; the pull exerted by surface tension accordingly is about 2 dyn when the wire dips in water and less than that with other liquids employed in our research. Variation of this force with temperature however only amounts, in the circumstances of the experiments, to a few hundredths of the total surface tension force on the wire. That is one part in 10^4 of the total measured forces (see Tables I–III); this systematic cause of error is thus of the same order of magnitude as other unavoidable random disturbances affecting our measurements. The improved quantitative agreement between experiment and theory relative to our previously published results is evidently due to the improvement of apparatus design and operation. The circumstance that experimental values still consistently fall below the corresponding ones calculated from Eq. (29) is however indicative of an inadequacy in some of the approximations adopted in the theory. Some of such inadequacies can be readily indicated.

A value of u_l higher than the adopted one—which was wave group velocity in the liquid at ultrasonic frequencies—would bring the calculated values in closer accord with experimental results. An increase in the value of u_l between 5% and 15% would bring most of the theoretical values in excellent agreement with measurement. Velocities of thermal phonon excitations in the Hz range, determined from Brillouin-scattering experiments, however, are generally only 2–8 % higher than the corresponding ultrasonic velocities. Propagation velocities at still higher frequencies are unfortunately unknown, corrections which should be introduced in the propagation velocities of the solid plungers also unknown. Finally it should be recalled that in the calculated value of the thermal-radiation force, the possible contribution of forces acting on the lateral surface of the plunger was neglected.

There is no need to discuss here any further the experiments of thermal diffusion, whose results were compared with the theory, since their critical survey can be found in the literature cited therein.

In conclusion, the experiments described above lend strong support to the proposed theory of thermal-radiation forces in the condensed phases. All the main theoretical predictions were confirmed. Indeed in the case of the experiments with the solid plungers (i) the forces measured were proportional to the difference of the k/u ratios of the liquid and solid medium: (ii) proportionality of the forces to the intensity of the temperature gradient was also ascertained; (iii) average temperature affects the results as forseen from the temperature dependence of the k/u of the materials; (iv) the sense of thermal-radiation forces depends, as expected, from the order of succession of the media along the temperature gradient.

In nonisothermal solutions, the thermodiffusive behavior of various kinds of solutes gives evidence of the action of forces that have each of the characteristics listed above under points (i)–(iv). This does not merely add independent supporting evidence to the experiments with macroscopic plungers, but shows that the concept of thermal-radiation force can be also applied to molecules and ions in a nonisothermal liquid medium. These forces act on every particle with which thermal excitations can exchange momentum. The quantitative agreement between theory and experiment is also quite encouraging, in view of the many unavoidable approximations introduced in the treatment.

Our treatment assumes that the material system dealt with consists of condensed phases. This circumstance was explicitly invoked at the beginning of Sec. II; it is also implicit wherever reference is made to phonon-type thermal excitations, not existent in the gaseous state. However some related problems arising in heat conducting gases, were analyzed showing that a heat flux produces forces on small suspended particles [43]. The argument used is gas kinetic and cannot be extended to the condensed phases. It should be remembered indeed that all attempts to interpret thermal diffusion in liquid solutions by means of adaptations of gas-kinetic or Brownian-motion models [44–47] were unable to yield satisfactory quantitative—or even qualitative—explanations of the observed phenomenology [16].

The field of thermal-radiation effects is very broad and much more experimentation will be necessary before the theory can be considered really established. Thermal diffusion, thermodyalysis, the Dufour effect, the behavior of high-temperature plasmas, acoustic streaming, and the Rayleigh-Bénard instabilities, as well as low-temperature phenomena such as the Kapitza fountain effect, just to mention a few examples, shall all have to be reexamined. Finally it is interesting to observe that in this paper only systems constituting of particles with short-range forces and possessing no long-range order have been considered. The application of the fundamental principle of momentum conservation leads to the discovery of new properties of the energy current and stress tensor in the nonisothermal state, because of the intrinsic anisotropy of such states. The widely accepted assumption is that a seemingly small departure from equilibrium, such as that caused by the introduction of a moderate temperature gradient, should not give rise to nonlinear effects. The present work suggests that such an assumption might not be justified.

Notwithstanding the relatively small intensity of thermal-radiation forces their study may thus prove to have sufficient theoretical and practical importance to justify further research in this neglected field.

APPENDIX

We refer to the system represented in Fig. 1—which we consider to be in steady-state conditions. It consists

of a series of anharmonic oscillators, constituted by normal sections interacting with the neighboring ones, occupying nonuniformly-spaced rest positions. Thermal expansion is seen as a nonuniformity of the numerical density of normal sections along x. (Obviously the section mass density, i.e., the number of molecules per section, increases going from the warmer to the cooler end.) Total oscillator energy varies along x in consequence of the existence of the temperature gradient.

We will now consider two molecules in the medium; let the force law be of the kind

$$f=\alpha r+\alpha\epsilon r^2 \text{ with } \epsilon r\ll 1 . \tag{A1}$$

Then at uniform temperature it is [48]

$$\langle r\rangle_\tau\cong h_0+\frac{\epsilon}{\alpha}k_BT , \tag{A2}$$

h_0 being the mechanical equilibrium position of one molecule (at 0 K) and where k_B is the Boltzmann constant. We assume the vibrations to be of small amplitude so that damping terms can be neglected.

The temperature gradient, of course, is applied along x; accordingly for the average position h_0 (averaged over the oscillator period), we may write

$$h_j\equiv\langle x_j\rangle_{\tau_j}\cong h_0+\frac{\epsilon}{\alpha}k_BT_j \tag{A3}$$

and hence

$$h_j-h_{j-1}\cong\frac{\epsilon}{\alpha}k_B(T_j-T_{j-1}) , \tag{A4}$$

$$h_{j+1}-h_j\cong\frac{\epsilon}{\alpha}k_B(T_{j+1}-T_j) . \tag{A5}$$

Equations (4A) and (5A) serve to simplify the equation of motion of the jth section

$$m\xi_j=\alpha(\xi_{j+1}-\xi_j)-\alpha(\xi_j-\xi_{j-1}) +\alpha\epsilon[(\xi_{j+1}-\xi_j)^2-(\xi_j-\xi_{j-1})^2] , \tag{A6}$$

where m is the mass and ξ_j the instantaneous displacement of the section. Under the condition $\epsilon r\ll 1$ of weak nonlinearity of the force law, and in the presence of a moderate temperature gradient, Eq. (5) of point (2) constitutes a good approximation.

Now we can develop $\xi_{j+1}-\xi_j$ and $\xi_j-\xi_{j-1}$ as

$$\xi_{j+1}-\xi_j=(h_{j+1}-h_j)\frac{\partial\xi_j}{\partial x}+\frac{1}{2}(h_{j+1}-h_j)^2\frac{\partial^2\xi_j}{\partial x^2}+\cdots , \tag{A7}$$

$$\xi_j-\xi_{j-1}=(h_j-h_{j-1})\frac{\partial\xi_j}{\partial x}-\frac{1}{2}(h_j-h_{j-1})^2\frac{\partial^2\xi_j}{\partial x^2}+\cdots , \tag{A8}$$

upon substitution in (6a) under (4A) and (5A), and neglecting terms higher than second order, we get

$$\frac{\partial^2\xi_j}{\partial t^2}=\frac{(\epsilon k_B)^2}{2\alpha m}[(T_{j+1}-T_j)^2+(T_j-T_{j-1})^2]\frac{\partial^2\xi_j}{\partial x^2} , \tag{A9}$$

with $T_{j+1}-T_j\cong T_j-T_{j-1}$. On the other hand

$$T_{j+1}-T_j=h_0\frac{dT_j}{dx}+\frac{1}{2}h_0^2\frac{d^2T_j}{dx^2}+\cdots , \tag{A10}$$

$$T_j-T_{j-1}=h_0\frac{dT_j}{dx}-\frac{1}{2}h_0^2\frac{d^2T_j}{dx^2}\cdots . \tag{A11}$$

Substituting (10A) and (11A) into (9A) and neglecting terms higher than second order, we get

$$\frac{\partial^2\xi_j}{\partial t^2}=\frac{(\epsilon k_B)^2}{\alpha m}\left[h_0\frac{dT_j}{dx}\right]^2\frac{\partial^2\xi_j}{\partial x^2} . \tag{A12}$$

Proceeding now to a continuum, one obtains

$$\frac{\partial^2\xi_x}{\partial t^2}=h_0^2\omega^2(x)\frac{\partial^2\xi_x}{\partial x^2} , \tag{A13}$$

having set

$$\omega^2(x)\equiv\frac{\epsilon^2}{\alpha m}\left[\frac{d}{dx}(k_BT)\right]^2 .$$

This is an interesting expression insomuch as Eq. (13A) can be identified with the d'Alembert wave equation of acoustics, for propagation along x. We assume sound velocity $u=u(x)$ to be coincident with $h_0\omega$, where $\omega=\omega(x)$ is angular frequency of the oscillator, physically constituted by the normal section through x. It should be observed that the "velocity" term

$$u(x)=[h_0^2\omega^2(\xi)]^{1/2}=\frac{h_0\epsilon}{(\alpha m)^{1/2}}\frac{d}{dx}(k_BT)$$

is not the usual propagation velocity of acoustic energy, depending only on equilibrium quantities. The "perturbation" we are dealing with in this context arises in the medium, due to the presence of the temperature gradient, and is connected with the nonuniformity of vibrational energy density along the x axis.

Since $\omega=2\pi/\tau$, it finally results that

$$\tau=2\pi h_0\frac{1}{u} . \tag{A14}$$

One could suspect that by neglecting in Eq. (6A) terms higher than second order, we have neglected altogether the anharmonicity of the chain of oscillators (the third term indeed disappears). This is not true, since anharmonicity is included in the calculations through h_j-h_{j-1} and $h_{j+1}-h_j$.

[1] J. W. Rayleigh, Philos. Mag. **3**, 338 (1902).
[2] J. W. Rayleigh, Philos. Mag. **10**, 364 (1905).
[3] L. Brillouin, Ann. Phys. **4**, 528 (1925).
[4] L. Brillouin, Rev. Acoust. **5**, 99 (1936), and references cited therein.
[5] R. Lucas, J. Phys. **8**, 410 (1937).
[6] F. Bopp, Ann. Phys. (Leipzig) **38**, 495 (1940).
[7] F. E. Borgnis, Rev. Mod. Phys. **25**, 653 (1953).
[8] L. Brillouin, J. Phys. Radium, **17**, 379 (1956).
[9] A. Johansen, J. Phys. Radium, **17**, 400 (1956).
[10] F. P. Bretherton, Lect. Appl. Math. **13**, 61 (1971).
[11] J. A. Rooney and W. L. Nyborg, Am. J. Phys. **40**, 1825 (1972).
[12] C. Truesdell and W. Noll, *Handbuch der Physik III/3,* edited by S. Flugge (Springer-Verlag, New York, 1974).
[13] F. S. Gaeta, Phys. Rev. **182**, 289 (1969).
[14] G. Brescia, E. Grossetti, and F. S. Gaeta, Nuovo Cimento, B **8**, 329 (1972).
[15] F. S. Gaeta, D. G. Mita, G. Perna, and G. Scala, Nuovo Cimento **30**, 153 (1975).
[16] F. S. Gaeta and A. Di Chiara, J. Polym. Sci. **13**, 163 (1975).
[17] F. S. Gaeta, G. Scala, G. Brescia, and A. Di Chiara, J. Polym. Sci. Polym. Phys. Ed. **13**, 177 (1975).
[18] F. S. Gaeta, G. Perna, and G. Scala, J. Polym. Sci. **13**, 203 (1975).
[19] F. S. Gaeta and D. G. Mita, J. Membr. Sci. **3**, 191 (1978).
[20] F. S. Gaeta and D. G. Mita, J. Phys. Chem. **83**, 2276 (1979).
[21] F. S. Gaeta, G. Perna, G. Scala, and F. Bellucci, J. Phys. Chem. **86**, 2967 (1982).
[22] D. G. Mita, F. Bellucci, M. G. Cutuli, and F. S. Gaeta, J. Phys. Chem. **86**, 2975 (1982).
[23] N. Pagliuca, D. G. Mita, and F. S. Gaeta, J. Membr. Sci. **14**, 31 (1983).
[24] N. Pagliuca, U. Bencivenga, D. G. Mita, G. Perna, and F. S. Gaeta, J. Membr. Sci. **33**, 1 (1987).
[25] D. Jou, J. Casas-Vasquez, and G. Lebon, Rep. Progr. Phys. **51**, 1105 (1988).
[26] D. D. Joseph and L. Preziosi, Rev. Mod. Phys. **61**, 41 (1989).
[27] L. Brillouin, *Les Tenseurs en Mécanique et en Élasticité,* edited by Masson et Cie (Paris, 1949).
[28] I. L. Fabelinskii, Usp. Fiz. Nauk. **77**, 649 (1962) [Sov. Phys. Usp. **5**, 667 (1963)].
[29] G. B. Benedek, J. B. Lastovka, K. Fritsch, and T. Greytak, J. Opt. Soc. Am. **54**, 1284 (1964).
[30] R. Y. Chiao and B. P. Stoicheff, J. Opt. Soc. Am. **54**, 1286 (1964).
[31] D. I. Mash, V. S. Starunov, and I. L. Fabelinskii, Zh. Eksp. Teor. Fiz. **47**, 783 (1964). [Sov. Phys. JETP **20**, 523 (1965)].
[32] W. J. Cowley, Contemp. Phys. **4**, 15 (1962).
[33] S. E. A. Hakim and W. J. Cowley, Nature **208**, 1082 (1965).
[34] F. S. Gaeta, E. Ascolese, U. Bencivenga, D. G. Mita, J. Ortiz de Zárate, N. Pagliuca, G. Perna, and S. Rossi (unpublished).
[35] L. D. Landau and E. M. Lifshitz, *Fluid Mechanics* (Pergamon, New York, 1959).
[36] A. H. Emergy Jr. and H. G. Drickamer, J. Chem. Phys. **23**, 2252 (1955).
[37] P. Debye and A. M. Bueche, *High Polymer Physics,* (Chemical, New York, 1948), pp. 497–527.
[38] G. Langhammer, Naturwissenschaften **41**, 525 (1954).
[39] G. Langhammer and K. Quitzsch, Macromol. Chem. **17**, 74 (1955).
[40] G. Langhammer, Kolloid **44**, 146 (1956).
[41] G. Langhammer, J. Chem. Phys. **54**, 885 (1957).
[42] A. Bierlein, C. R. Finch, and H. E. Bowers, J. Chem. Phys. **54**, 873 (1957).
[43] H. Vestner and L. Valdmann, Physica A **86**, (1977).
[44] Th. Wereide, Ann. Phys. **2**, 67 (1914).
[45] S. Chapman, Proc. R. Soc. London, Ser. A **119**, 34 (1928).
[46] S. Chapman, Proc. R. Soc. London, Ser. A **119**, 55 (1928).
[47] G. Nicolis, J. Chem. Phys. **43**, 1110 (1965).
[48] I. G. Main, *Vibration and Waves in Physics* (Cambridge University Press, London, 1978).